Title

Investigation of surface effects through the application of the functional binders in lithium sulfur batteries

Authors

Ai, Guo
Dai, Yiling
Ye, Yifan
et al.

Publication Date

2015-09-01

DOI

10.1016/j.nanoen.2015.05.036

Peer reviewed

Investigation of surface effects through the application of the functional binders in lithium sulfur batteries

Guo Ai[a,b], Yiling Dai[a], Yifan Ye[c,d], Wenfeng Mao[a], Zhihui Wang[a], Hui Zhao[a], Yulin Chen[a], Junfa Zhu[d], Yanbao Fu[a], Vincent Battaglia[a], Jinghua Guo[c], Venkat Srinivasan[a], Gao Liu[a*]

[a]*Environmental Energy Technologies Division, Lawrence Berkeley National Laboratory, Berkeley, California 94720, United States*

[b]*Science and Technology on Reliability Physics and Application of Electronic Component Laboratory, No. 5 Electronic Research Institute, Guangzhou 510610, China*

[c]*Advanced Light Source, Lawrence Berkeley National Laboratory, Berkeley, California 94720, United States*

[d]*National Synchrotron Radiation Laboratory and Collaborative Innovation Center of Suzhou Nano Science and Technology, University of Science and Technology of China, Hefei, Anhui 230029, China*

[*] Tel.: +1-510-486-7207; fax: +1-510-486-7303; Email: gliu@lbl.gov (G. Liu)

Abstract

Sulfur species dissolution and phase transformation during the charge and discharge process strongly affects lithium sulfur (Li-S) battery performance. Interface properties play an important role in these batteries. In this work, four kinds of binders with different chemical and electrical properties were employed to study how the interface properties affect the battery reaction mechanism. The phase transformation of sulfur species was studied in detail. Remarkable differences were observed among cathodes with different binders. More solid-phase sulfur precipitation was observed with binders that have carbonyl functional groups, like poly(9, 9-dioctylfluorene-co-fluorenone-co-methylbenzoic ester) (PFM) and poly(vinylpyrrolidone) (PVP), in both fully charged and discharged states. Also, the improved conductivity from introducing conductive binders greatly promotes sulfur species precipitation. These findings suggest that the contributions from functional group affinity and binder conductivity lead to more sulfur transformation into the solid phase, so the shuttle effect can be greatly reduced, and better cell performance can be obtained.

Keywords

Li-S battery; Conductive binder; Surface effect; Self-discharge; Binding energy

1. Introduction

Li-S batteries have attracted a great amount of attention due to their extremely high theoretical specific capacity, low cost, and environmental benignity[1-5]. However, they also have a few shortcomings, such as relatively poor cycling life, low columbic efficiency, and high self-discharge loss, which have hindered its practical application. These limitations mainly result from the low conductivity of the solid products (S_8 and Li_2S)[5, 6] and the shuttle effect of the dissolved lithium polysulfide in the electrolyte[7, 8]. It is well known that Li-S batteries are noted for phase transformation during cycling. In a Li-S cathode composed of non-encapsulated sulfur particles, conductive additive (acetylene black, AB), and polymer binder, the sulfur dissolves as polysulfide and precipitates as elemental sulfur or lithium sulfide during cycling. In discharge processes, solid-phase S_8 dissolves into soluble Li_2S_x(x=2-8) and then precipitates to solid-phase Li_2S. Correspondingly, in charge processes, Li_2S gradually dissolves into soluble polysulfide and then returns to solid-phase S_8 or long-chain polysulfide Li_2S_8[9]. During both charge and discharge processes, the electrode provides a conductive matrix for the solid sulfur species to precipitate. The matrix surface chemistry determines the bonding between the matrix and the precipitated sulfur species, so a strong bonding can help fix sulfur species to the cathode matrix. This fixation can reduce the polysulfide shuttle effect and improve long-term performance stability. AB is generally used as conductive additive in the conductive matrix, but some research shows that the binding energy between solid sulfur species and AB is very low, and possible detachment of solid sulfur species from AB might exist[10]. However, since the particle surface of AB is covered by the polymer binders to form the matrix, the predominate surfaces for sulfur species precipitation are the polymer binders[11, 12]. Therefore the surface effect of the binders on the battery reaction is a crucial issue in improving the performance of Li-S batteries.

Different kinds of polymer binders have been applied in Li-S batteries. Early works mainly focus on non-conductive polymers as binders; these include poly(vinylidenedifluoride) (PVDF)[13, 14], poly(vinylpyrrolidone) (PVP)[11], gelatin[15], styrene-butadiene rubbers (SBR)[16], and others. They mainly act as binding agents to glue the active material and conductive additives together and maintain the integrity of the electrode. Recently, conductive binders have been introduced into the battery system, and a noted improvement in battery performance was obtained[17-19]. The conductive binders can act as both the binding agents and the conductive framework in Li-S batteries. The most well-known conductive binder is poly(3,4-ethylenedioxythiophene):polystyrene sulfonate (PEDOT:PSS, written as PEDOT for short in this paper)[19], which is also widely used in photovoltaic and photoelectronic devices. It shows much improved performance over non-conductive binders in Li-S batteries[20]. Still, a detailed understanding of how conductive binders can improve battery performance needs to be investigated.

In this work, four kinds of binders with different functional groups and conductive properties were employed to study how the interface chemical properties and binder conductivity affected the battery reaction mechanism. Poly(9,9-dioctylfluorene-co-fluorenone-co-methylbenzoic ester, PFM for short) was specially designed and synthesized in our group[17, 18]. It had two carbonyl groups and was highly conductive. It also had a high binding energy with sulfur species (Li_2S_x, x=1-8) through incorporation of the fluorenone carbonyl (C=O) group and methylbenzoic ester-$PhCOOCH_3$ (MB) group and showed superior performance in Li-S batteries. Thus, PFM was selected to illustrate the importance of both the functional groups and the conductive properties of binders on battery performance. The second binder introduced in this work was a well-known conductive binder, PEDOT. Between PFM and PEDOT, we could compare the influence of functional groups on the cell reaction mechanism when both binders were

conductive. The third binder we introduced was a non-conductive PVP polymer, which has an amide carbonyl functional group and a high binding energy with Li_2S_x (x=1-8)[11]. By comparing the performance between PFM and PVP, we could demonstrate how the binder's electronic conductivity could improve the performance of the cell when they both had a carbonyl group to assist sulfur species precipitation. PVDF, the most commonly used non-conductive binder for both lithium-ion and Li-S batteries, was studied for comparison. By closely comparing the difference in morphology and structure of sulfur species after cycling, our work suggested that the binders have a great influence on battery performance through surface modification. With the assistance of the carbonyl group and high conductivity of the binder, more solid products (S in charged state, and then Li_2S in discharged state) was observed and suppression of polysulfide dissolution was obtained. This provided us a new direction to design a novel conductive binder and electrode matrix to further improve Li-S battery performance.

2. Experimental

2.1 Materials

The micrometric sulfur powder was purchased from Mallinckrodt Company, and acetylene black was purchased from Denka Japan. Four binders were used in this work, and PFM was synthesized according to previous work[17]. The PEDOT and PVP were purchased from Sigma-Aldrich Inc. The PVDF was purchased from Kureha America, Inc. The N-methyl-2-pyrrolidone (NMP) (anhydrous, 99.5%) was purchased from Sigma-Aldrich Inc. and used as the solvent for laminate with PVP and PVDF as binder. The chlorobenzene (Sigma-Aldrich Inc.) was used as the solvent for PFM. The electrolyte for cell testing was composed of 1 M lithium salt bis(trifluoromethanesulfonyl)imide (LiTFSI) dissolved in polyethylene glycol dimethyl ether (PEGDME), and 1 wt% $LiNO_3$, all purchased from Sigma-Aldrich. The molecular weight of the PEGDME was around 500 daltons.

2.2 Cathode fabrication

The PVP and PVDF were first dissolved in NMP, while PFM was dissolved in chlorobenzene, and PEDOT was diluted by de-ionized water, all at 5 wt% ratio. Commercial micrometric sulfur powder and AB were added into the binder-solvent solution after the binder was thoroughly dissolved. The weight ratio of these three components was: 50% sulfur, 10% binder, and 40% AB. The mixture was mixed by a ball-milling method overnight to obtain uniform slurry. The laminate was then made by coating the slurry on an 18-μm-thick battery-grade aluminum current collector with a Mitutoyo doctor blade and an Elcometer motorized film applicator. Typical mass loading of sulfur was 0.3 mg/cm^2. After the laminate was fully dried, it was further dried in a vacuum oven at 50 °C overnight.

2.3 Cell assembly and testing

Li-S batteries were tested with 2325-type coin cells (National Research Council Canada). The cells were assembled in an argon-filled glove box with oxygen content less than 0.1 ppm. The size of the sulfur electrode was 1/2-inch OD, and the size of the counter electrode lithium metal disk was 11/16-inch OD. The Li foil was purchased from FMC-Lithium Co. The separator used was polypropylene film (Celgar 2400). Galvanostatic cycling tests were performed on a Maccor series 4000 cell tester (Maccor, Inc., Tulsa, OK). The voltage window was 1.5–2.6 V. The cells were cycled at C/10 for 10 cycles to get a relatively stable performance. After the first 10 cycles, the self-discharge test was performed by charging

the cells to the fully charged state and then letting them rest for 60 hours. This procedure was repeated twice, with the third rest lasting 240 hours. With this cycling procedure, both the cycling performance for the cathodes and the self-discharge retention ability could be obtained.

2.4 Material characterization techniques

Morphology of the electrode surface was characterized with a JSM-7500F scanning electron microscope at the National Center for Electron Microscopy (NCEM) at Lawrence Berkeley National Laboratory. The cycled Li-S batteries were opened with a cell opener, and the electrode was washed thoroughly with 1,3-dioxolane/1,2-dimethoxyethane (DOL/DME) with a volume ratio of 1:1 inside an argon-filled glove box.

For the total fluorescence yield near-edge X-ray absorption fine structure (TFY-NEXAFS) experiments, the cells were disassembled in fully discharged state after cycling for 50 cycles and washed with DOL/DME 1:1 solution thoroughly in the glove box. The samples were well sealed using 2.53 micrometer-thick Kapton film. The S K-edge X-ray absorption spectra were collected at beam line 9.3.1, 10.3.2 at Lawrence Berkeley National Laboratory's Advanced Light Source,. This was a bending magnet beam line with photon energies ranging from 2320 to 5600 eV (9.3.1) and 2400 to 17000 eV (10.3.2) and an unfocused beam size of 1 mm*0.7 mm (9.3.1) and 20 μm*16 μm (10.3.2). Total fluorescence signals were collected with a channeltron with an approximately 0.36 eV resolution. The photon incident angle was set at 45^{o} for all samples. Probing depth of up to a few microns could be achieved.

3. Results and discussion

3.1 Cycling and self-discharge performance of cathodes with different binders

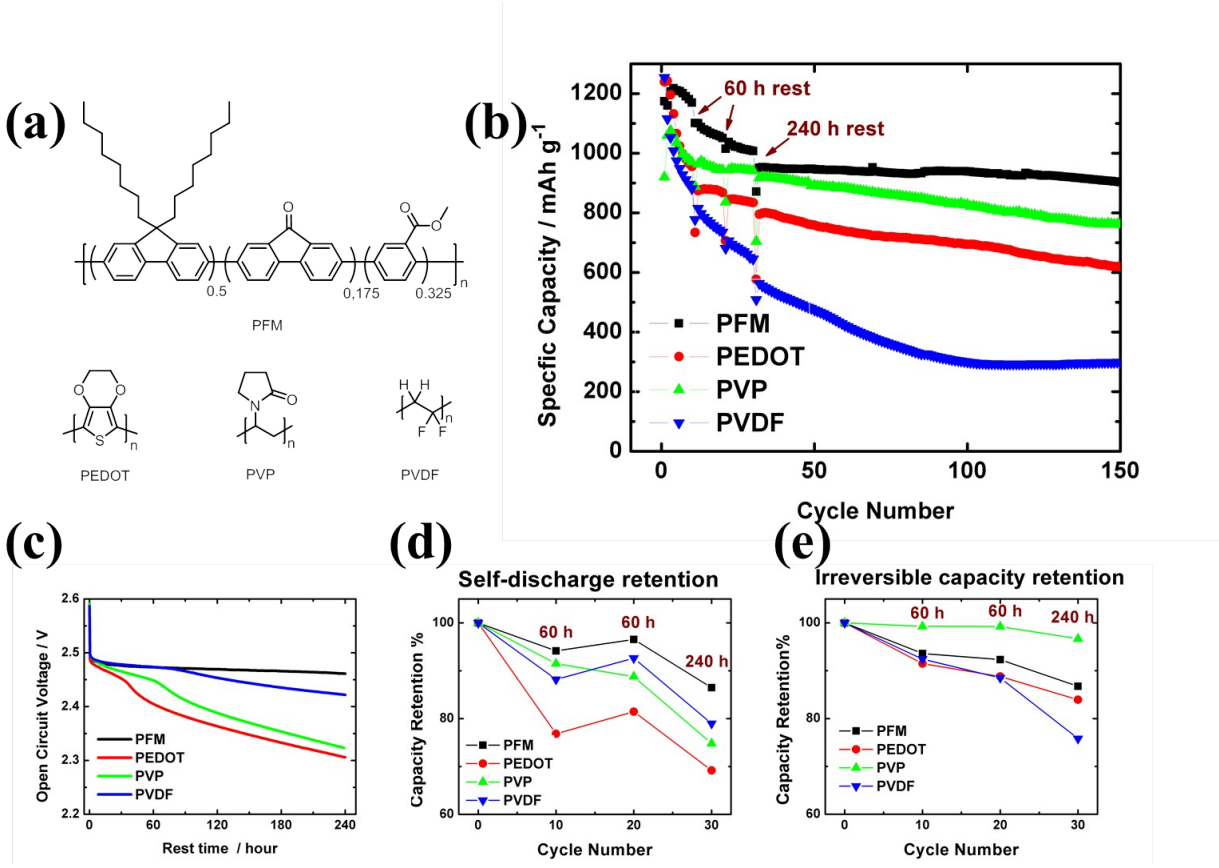

Figure 1 (a) Chemical structures of the four different binders: PFM, PEDOT, PVP, and PVDF. (b) Cycling performance at C/10 and self-discharge performance of cathodes with different binders. (c) The open circuit voltage change vs. rest time during the third self-discharge rest of 240 hours for the PFM-S, PEDOT-S, PVP-S, and PVDF-S cathodes. The self-discharge capacity retention ratio (d) and irreversible capacity retention ratio (e) for cathodes with different binders during the self-discharge test.

In this work, four binders were introduced to study the surface effect in Li-S battery working mechanism. PFM and PEDOT are conductive binders, while PVP and PVDF are non-conductive binders. The chemical structures for these four binders were shown in Figure 1a. PFM and PVP both had carbonyl groups, while PEDOT and PVDF did not. The cycling test was designed by regular cycling procedures with three self-discharge tests as intervals. The 60h, 60h, and 240h self-discharge tests were set after the tenth, twentieth, and thirtieth cycles. This could show both the cycling performance and the self-discharge prevention ability for four cathodes with different binders, named PFM-S, PEDOT-S, PVP-S and PVDF-S for short. As shown in Figure 1b, each cathode showed almost the same specific capacity at the first few cycles, but the PFM-S showed the smallest decay in the following cycling test. With the help of the relatively good conductivity, the PEDOT-S showed good performance, but the capacity decay was larger than that of PFM-S. Among all cathodes, the PVP-S showed the smallest capacity in the first few cycles, probably due to the incomplete reduction of sulfur wrapped by the non-conductive binder PVP at the beginning. The performance of PVP-S was better than that of PEDOT-S and inferior to that of PFM-S, indicating that both the high conductivity and the functional group of the binder were important to achieve high performance in the Li-S batteries.

The open circuit voltage drop for long time rest in the fully charged state was one of the most straightforward ways to show the self-discharge prevention ability. Figure 1c showed that during the 240-hour rest, PFM-S showed almost no voltage drop, while the other three cathodes (PEDOT-S, PVP-S, and PVDF-S) showed clear voltage drops. The open circuit voltage was closely related to the difference in resultant sulfur species in fully charged state and in their reaction activity. The voltage indicated that some chemical reactions occurred spontaneously during the self-discharge rest in these three cells. This will be discussed in the next section.

The self-discharge retention ability of cathode could also be characterized by two other factors. One is the self-discharge capacity retention Q_{sd}, which shows the capability of the cell to maintain its capacity during the rest in its fully charged state.

$$Q_{sd} = \frac{C_a}{C_b}$$

C_a is the discharge capacity after rest; C_b is the discharge capacity before rest.

The other factor is the irreversible capacity retention Q_{ir}, which shows the ratio of capacity that could be recovered after self-discharge rest.

$$Q_{ir} = \frac{C_f}{C_b}$$

C_f is the discharge capacity of the following cycle after rest; C_b is the discharge capacity before rest.

The self-discharge performance was plotted in Figure 1d and 1e. The self-discharge capacity loss in Figure 1d is plotted by the loss of each rest period. The irreversible capacity loss in Figure 1e is plotted by the sum of the loss from the former rest period. The capacity loss from cycling was not included in these two factors. In addition, we note that the capacity retention for the second 60-hour test loss is smaller than the first 60-hour test for all four samples, probably due to the smaller side reaction and relatively stable performance after more cycles. The PFM-S showed a small capacity fade during all three self-discharge tests compared to PEDOT-S and PVDF-S. The irreversible capacity loss for PVP-S was the smallest among the four. This indicated that in the PFM-S most of the sulfur species had precipitated into the solid phase, and that it had the best capability in keeping the active material from self-discharge. However, in the other three, since most of the sulfur species existed as dissolved species in the electrolyte, they tended to react spontaneously into a shorter-chain polysulfide. This will be discussed in a later section.

3.2 Morphology of cathodes with different binders in charged and discharged state

To study the mechanism of the surface effect of different binders on cycling performance, the cells were disassembled, both in charged and discharged states, and the cathodes were thoroughly washed for the morphology study. As shown in Figure 2 and 3, enormous differences in morphology could be observed for these electrodes, both in the charged state and the discharged state, indicating different amounts of solid sulfur species precipitation[9, 21]. It should be noted that more solid product precipitation was observed for PFM-S, both in the charged and discharged states. In addition, the cathodes with conductive binders exhibit more uniform precipitation morphologies than those with non-conductive ones. This

suggested that surface properties were modified by the binders and solid-phase product precipitation was influenced by the affinities between the binders and Li_2S.

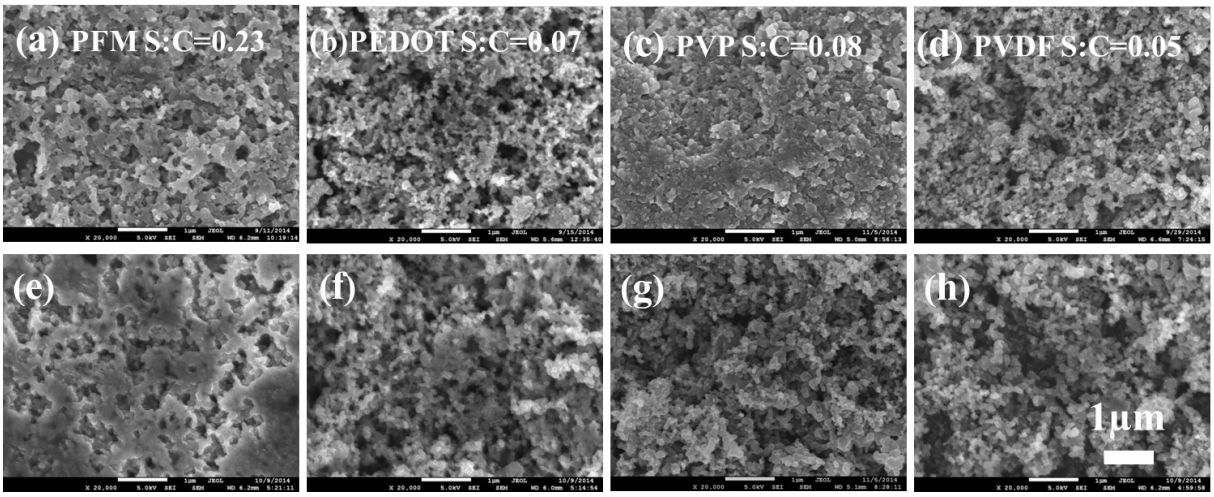

Figure 2 SEM images of the top and bottom morphology of PFM-S(a), (e); PEDOT-S(b), (f); PVP-S(c), (g); PVDF-S(d), (h) in fully charged state. All SEM images have the same magnification in this figure.

When the cells were disassembled in fully charged state, both the electrode integrity and the appearance were totally different for cathodes with different binders, as shown in Figure S1. During the cell disassembly and washing process, the appearance of the PFM-S remained unchanged, and almost none of the reddish electrolyte could be seen in the opened cell. This indicated that in the fully charged state, the sulfur species could be precipitated as solid-phase sulfur, assisted by the PFM binder, which could help the PFM-S electrode maintain its integrity. The integrity of PVP-S was also good, but the PEDOT-S and PVP-S partially peeled off from the current collector, and the PVDF-S cathodes fragmented into small pieces. Correspondingly, a light reddish color electrolyte could be observed for PVP-S, while a deeper red electrolyte was observed for the PEDOT-S and PVDF-S. This suggests that for PEDOT-S and PVDF-S in fully charged state, the sulfur species remained dissolved in electrolyte as long-chain deep red polysulfide (Li_2S_8 or Li_2S_6), instead of precipitating as solid-phase sulfur. A more dissolved phase of polysulfide would result in a more severe shuttle effect, which has a negative influence on the cell performance.

The solid-phase sulfur precipitation in PFM-S and PVP-S cathodes could clearly be seen by SEM (Figure 2a, 2c). A layer of solid-phase substance was clearly observed coating the AB particle surface, which is the precipitated sulfur species. In comparison, for PEDOT-S and PVDF-S, almost none of this precipitation layer was observed (Figure 2b, 2d). This further supported the former suggestion that in fully charged state, the sulfur species precipitated as solid-phase sulfur in PFM-S and PVP-S, while in PEDOT-S and PVDF-S the sulfur species remained dissolved in electrolyte as long-chain polysulfide, which had a deep red color (Figure S1f, S1h). To further observe the solid-phase sulfur precipitation, the electrode laminate layer was peeled off from the current collector and observed from the bottom surface near the current collector. For PFM-S, as shown in Figure 2a and 2e, a large amount of solid-phase precipitation could be observed at the bottom; as much as on the surface. This indicated uniform precipitation of sulfur throughout the film, which was assisted both by the carboxyl group and the conductivity of the binder. For PVP-S, as much sulfur precipitation as was seen in PFM-S was observed on the surface (Figure 2c), but almost none was observed at the bottom (Figure 2g). The precipitated

sulfur on the top surface seemed to clog the pores and prevent the polysulfide from penetrating, which led to insufficient sulfur precipitation near the bottom, as well as polysulfide residues in the electrolyte. This could demonstrate the importance of binder conductivity in sulfur precipitation. With a much larger conductive surface area and the assistance of the carboxyl group in PFM-S, a more uniform sulfur precipitation could take place, and less polysulfide could be observed in the electrolyte. However, for PEDOT-S (Figure 2b, 2f) and PVDF-S (Figure 2d, 2h), no solid-phase precipitation was observed on AB, both at the electrode surface and at the bottom. This indicated that the carboxyl group was crucial for assisting solid-phase sulfur precipitation in the charged state. In addition, the relative ratio of sulfur to carbon calculated from EDX data could be used as a proof of sulfur existence. For PFM-S, the ratio of sulfur to carbon was 0.23, while a sulfur-to-carbon ratio of almost zero was observed in PEDOT-S and PVDF-S. The PVP-S only showed subtly more sulfur than PEDOT-S and PVDF-S.

With the above observation, the self-discharge restraining ability for different cathodes could be explained. The reactant tended to change spontaneously into lower energy products during the self-discharge test, and this process was greatly slowed when the reactant was in the solid phase. In the PFM-S cathodes, most of the sulfur species precipitated as solid phase in fully charged state, which lead to good self-discharge restraining ability and almost no change in open-circuit voltage during long rests. However, in PEDOT-S and PVDF-S, the sulfur species mainly dissolved in electrolyte as long-chain polysulfide, which tended to react spontaneously and can be observed as a drop in open-circuit voltage. Thus, a much larger self-discharge loss was observed in the cathodes when no carbonyl group was present.

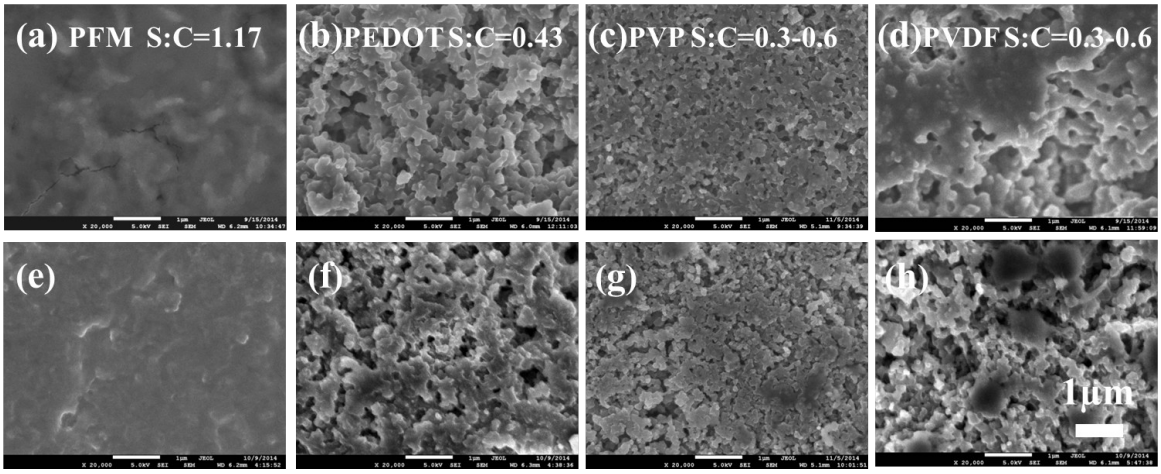

Figure 3 SEM images of the top and bottom morphology of PFM-S (a), (e); PEDOT-S (b), (f); PVP-S(c), (g); and PVDF-S (d), (h) in fully discharged state. All SEM images have the same magnification in this figure.

In fully discharged state, the four cathodes also exhibited differences in SEM morphology. To further observe the solid-phase Li_2S precipitation, the morphology of electrode laminate was observed both from the top surface (Figure 3a-3d) and the bottom of the laminate near the current collector (Figure 3e-3h). As shown in Figure 3a and 3e, a large amount of solid-phase Li_2S precipitation was observed for PFM-S; no pore was left void in the film, and the AB layer was totally buried. For PEDOT-S in Figure 3b and 3f, the Li_2S precipitation was a thin solid-phase layer uniformly coated on the surface of AB, indicating good conductivity of PEDOT. But due to the lower binding energy of PEDOT with Li_2S, the amount of precipitated Li_2S in PEDOT-S was less than that in PFM-S. In PVP-S in Figure 3c and 3g, the amount of

Li_2S precipitation was a little more than that in PEDOT-S, but less than that in the PFM-S. The carbonyl group in PVP-S had a high binding energy with Li_2S, which can assist Li_2S precipitation. Also, the polar nature of PVP helped facilitate Li_2S precipitation. But the surface area for Li_2S precipitation was limited by the poor conductivity of PVP, which is also the case in PVDF-S. Li_2S was non-uniformly distributed in PVP-S and PVDF-S (Figure 3d, 3h). In these cases, some active material might become isolated from the conductive network and be unable to participate in charge or discharge processes. This loose Li_2S layer could also be identified by the smaller overpotential on the PVDF-S voltage-capacity curve compared to that of PFM-S and PEDOT-S at the start of the charge region in Figure 5. This will be discussed in the next section. The ratios of sulfur to carbon derived from EDX data were 1.17 for PFM-S, 0.43 for PEDOT-S, and 0.3-0.6 (uneven) for PVP-S and PVDF-S, which indicated that far more Li_2S precipitated in PFM-S than in the others.

3.3 Near-edge X-ray absorption fine structure (NEXAFS) characterization of cathodes with different binders

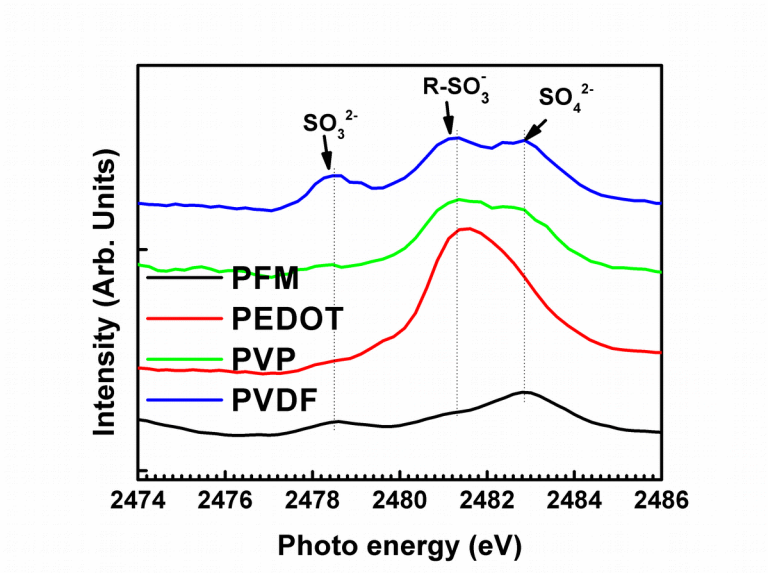

Figure 4 TFY-NEXAFS spectra of PFM-S, PEDOT-S, PVP-S, and PVDF-S cathodes in fully charged state.

NEXAFS is a sensitive technique to probe the chemical bonding and electronic structure of various systems (via the excitation of core electrons to the empty or partially filled states) [22-25]. In this work, S K-edge NEXAFS data were used to identify the S-related side reaction on the cathodes. The S K-edge TFY-NEXAFS data acquired on the samples of PFM-S, PEDOT-S, PVP-S, and PVDF-S were collected after 50 cycles at full charge. In Figure 4, the spectra were calibrated to the element sulfur located at 2472.2 eV. The side reaction product could be identified in the TFY-NEXAFS spectrum in the region of 2478.0-2485.0 eV. The peak at 2481.3 eV should be assigned to the side reaction assisted by the binder itself, with reaction product $R\text{-}SO_3^-$. The peak at 2481.3 eV should be assigned to the side reaction assisted by the binder itself, with reaction product $R\text{-}SO_3^-$. The peak at 2478.5 eV can be assigned to the transition of S 1s to the SO_3^{2-} σ* state and the 2482.8 eV peak can be assigned to the S 1s transition to the SO_4^{2-} σ* state, which indicated the side reaction products of the sulfur species with the electrolyte. The $R\text{-}SO_3^-$ peak is the weakest in PFM-S compared to those in the other three. There are much less binding

between binders and the sulfur oxidized species, which indicated that PFM has a positive effect in reducing the side reactions.

3.4 Surface reaction analysis through charge-discharge voltage profile

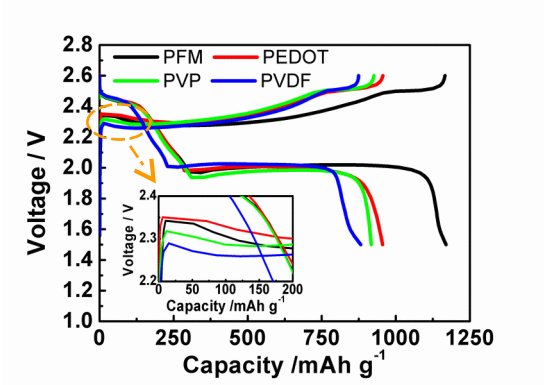

Figure 5. Voltage profile of the tenth cycle of PFM-S, PEDOT-S, PVP-S, and PVDF-S cathodes. Inset shows the detailed voltage curves at the beginning of the charge.

The charge-discharge voltage profile at the tenth cycle was used to analyze the detailed phase transformation during charge and discharge processes. As can be observed in Figure 5, the PFM-S, PEDOT-S, and PVP-S showed almost the same discharge characteristic in the upper voltage plateau region (2.6 V-1.95 V), which means the same amount of S_8/Li_2S_8 changed into dissolved state Li_2S_4. However, the voltage profile of the lower voltage plateau region (1.95 V-1.5 V) was different for these three electrodes: more capacity was obtained in PFM-S than in PEDOT-S and PVP-S. For PFM-S, 876 mAh/g capacity was obtained in the lower voltage plateau region, which was 69.7% of the theoretical capacity (1256 mAh/g). However, for PEDOT-S and PVP-S, only 668.5 mAh/g and 606.9 mAh/g capacity were obtained in the lower voltage plateau region, which was 53.2% and 48.3% of the theoretical capacity, respectively. This indicated that the PFM had a positive effect in assisting Li_2S precipitation. Two conclusions can be drawn from this result. First, the strong affinity between the carbonyl functional group of PFM and the sulfur species could assist solid-phase Li_2S precipitation. Second, a much larger conductive surface area of the conductive binder PFM helped to create more reaction sites for Li_2S precipitation. Although the same amount of dissolved state Li_2S_4 was obtained in PFM-S, PEDOT-S, and PVP-S in the upper voltage plateau region, the Li_2S precipitation in PFM-S was almost 30% higher than that in PEDOT-S and PVP-S in the lower voltage plateau region. Consequently, with PEDOT-S and PVP-S, there would be more residual sulfur species dissolved in the electrolyte, which would result in a more severe shuttle effect than with PFM-S. This was the reason that the PEDOT-S and PVP-S showed larger decay than PFM-S during cycling in Figure 1b. In the fully discharged state, the conductive matrix surface was covered by the solid-phase Li_2S layer. Furthermore, because of the poor conductivity of the Li_2S layer, only a very limited thickness of Li_2S could precipitate on the conductive surface before the layer turned highly resistive[6]. There is a characteristic over-charge peak at the beginning of the charge process, which was closely related to the Li_2S layer (Figure 4 inset). PVP-S and PVDF-S showed a smaller overpotential than PFM-S and PEDOT-S. This is because the cathodes of the non-conductive PVP and PVDF did not have large surface areas to assist Li_2S precipitation, so the precipitated Li_2S layer was thinner and inconsistent in PVP-S and PVDF-S, and might peel off or be isolated from conductive matrix [8, 22].

4. Conclusion

We have investigated the effects of both functional group and conductivity of polymer binders on the performance of Li-S batteries. Four different kinds of binders (PFM, PEDOT, PVP, and PVDF) were systematically studied and compared. Both the electrochemical performance analysis and the post-test analysis were conducted to explore how the polymers influence the electrochemical process. The electrodes with different binders showed significant differences in the morphology, compositions of sulfur species, and electrochemical characteristics. NEXAFS was also used to obtain the information about the interaction between the binder and side-reaction sulfur resultants.

PFM, which had the desired functional group and high conductivity, had the best cycling performance and self-discharge retention ability among all binders in this work. In both fully charged and discharged states, more solid sulfur species precipitation was observed in cathodes with binders that had carbonyl groups (PFM and PVP) than in cathodes with binders that did not have carbonyl groups (PEDOT and PVDF). This is because the carbonyl group's binding energy with the sulfur species was high, which greatly assisted the solid sulfur species precipitation during both the charge and discharge processes. This strong binding effect between the carbonyl group and the sulfur species might help to provide preferred reaction spots for solid-phase product precipitation. The solid-phase sulfur species precipitation would have a positive effect in reducing the shuttle effect, maintaining good self-discharge retention ability, and achieving long-term cycling stability. The electrical properties of the binders were also important. The conductive binders could provide the largest surface area for reactions to take place and effectively help the resistive solid-phase sulfur species participate in the reactions. In the tests with non-conductive binders, insufficient sulfur species dissolution and non-uniform precipitation were observed.

With a much larger and binding-assisted conductive surface to promote precipitation, PFM-S showed the largest amount of sulfur species precipitation among all the binders studied. These results suggest that both the functional group (the carbonyl group, in this case) and the conductivity of the binder played important roles in assisting the solid sulfur species precipitation (S_8 in charged state and Li_2S in discharged state), which was crucially important in reducing the shuttle effect and achieving good self-discharge and cycling performance in Li-S batteries. Therefore, an improved understanding of how the binder influences the cell performance will be helpful for the design of a better binder. Future design of binders for Li-S batteries will focus on these issues.

References

[1] D. Bresser, S. Passerini, B. Scrosati, Chemical Communications, 49 (2013) 10545.
[2] M. Barghamadi, A. Kapoor, C. Wen, Journal of the Electrochemical Society, 160 (2013) A1256-A1263.
[3] P.G. Bruce, S.A. Freunberger, L.J. Hardwick, J.-M. Tarascon, Nature Materials, 11 (2011) 19-29.
[4] X. Ji, S. Evers, R. Black, L.F. Nazar, Nature Communications, 2 (2011) 325.
[5] Y. Yang, G. Zheng, Y. Cui, Chemical Society Reviews, 42 (2013) 3018.
[6] Y. Yang, G. Zheng, S. Misra, J. Nelson, M.F. Toney, Y. Cui, Journal of the American Chemical Society, 134 (2012) 15387-15394.
[7] Y.V. Mikhaylik, J.R. Akridge, Journal of The Electrochemical Society, 151 (2004) A1969.
[8] S. Evers, T. Yim, L.F. Nazar, The Journal of Physical Chemistry C, 116 (2012) 19653-19658.

[9] M. Cuisinier, P.-E. Cabelguen, S. Evers, G. He, M. Kolbeck, A. Garsuch, T. Bolin, M. Balasubramanian, L.F. Nazar, The Journal of Physical Chemistry Letters, 4 (2013) 3227-3232.
[10] G. Zheng, Q. Zhang, J.J. Cha, Y. Yang, W. Li, Z.W. Seh, Y. Cui, Nano Letters, 13 (2013) 1265-1270.
[11] Z.W. Seh, Q. Zhang, W. Li, G. Zheng, H. Yao, Y. Cui, Chemical Science, 4 (2013) 3673.
[12] H. Yao, G. Zheng, P.-C. Hsu, D. Kong, J.J. Cha, W. Li, Z.W. Seh, M.T. McDowell, K. Yan, Z. Liang, V.K. Narasimhan, Y. Cui, Nature Communications, 5 (2014).
[13] L. Chen, L.L. Shaw, Journal of Power Sources, 267 (2014) 770-783.
[14] Z. Lin, C. Liang, Journal of Materials Chemistry A, 3 (2015) 936-958.
[15] Y. Wang, Y. Huang, W. Wang, C. Huang, Z. Yu, H. Zhang, J. Sun, A. Wang, K. Yuan, Electrochimica Acta, 54 (2009) 4062-4066.
[16] M.-K. Song, Y. Zhang, E.J. Cairns, Nano Letters, 13 (2013) 5891-5899.
[17] G. Liu, S. Xun, N. Vukmirovic, X. Song, P. Olalde-Velasco, H. Zheng, V.S. Battaglia, L. Wang, W. Yang, Advanced Materials, 23 (2011) 4679-4683.
[18] M. Wu, X. Xiao, N. Vukmirovic, S. Xun, P.K. Das, X. Song, P. Olalde-Velasco, D. Wang, A.Z. Weber, L.-W. Wang, V.S. Battaglia, W. Yang, G. Liu, Journal of the American Chemical Society, 135 (2013) 12048-12056.
[19] W. Li, Q. Zhang, G. Zheng, Z.W. Seh, H. Yao, Y. Cui, Nano Letters, 13 (2013) 5534-5540.
[20] Z. Wang, Y. Chen, V. Battaglia, G. Liu, Journal of Materials Research, 29 (2014) 1027-1033.
[21] M.A. Lowe, J. Gao, H.D. Abruña, RSC Advances, 4 (2014) 18347.
[22] X. Feng, M.-K. Song, W.C. Stolte, D. Gardenghi, D. Zhang, X. Sun, J. Zhu, E.J. Cairns, J. Guo, Physical Chemistry Chemical Physics, 16 (2014) 16931.
[23] T. Takeuchi, H. Kageyama, K. Nakanishi, Y. Inada, M. Katayama, T. Ohta, H. Senoh, H. Sakaebe, T. Sakai, K. Tatsumi, H. Kobayashi, Journal of The Electrochemical Society, 159 (2012) A75.
[24] T.A. Pascal, K.H. Wujcik, J. Velasco-Velez, C. Wu, A.A. Teran, M. Kapilashrami, J. Cabana, J. Guo, M. Salmeron, N. Balsara, D. Prendergast, The Journal of Physical Chemistry Letters, 5 (2014) 1547-1551.
[25] A. Vairavamurthy, Spectrochimica Acta Part A: Molecular and Biomolecular Spectroscopy, 54 (1998) 2009-2017.

ACKNOWLEDGEMENTS

This work was funded by the Assistant Secretary for Energy Efficiency, Office of Vehicle Technologies of the U.S. Department of Energy (U.S. DOE) under contract no. DE-AC02-05CH 11231 under the Advanced Battery Materials Research (BMR) program. The authors acknowledge support of the National Center for Electron Microscopy at the Lawrence Berkeley National Laboratory, which is supported by the U.S. Department of Energy under Contract # DE-AC02-05 CH11231. The work at the Advanced Light Source is supported by the Office of Basic Energy Sciences, of the U.S. Department of Energy under Contract No. DE-AC02-05CH11231. Junfa Zhu thanks the financial support from the National Natural Science Foundation of China (U1232102). Thanks Jing Wang for the modification of the manuscript. Also, Guo Ai and Wenfeng Mao are supported by the China Scholarship Council.

TOC

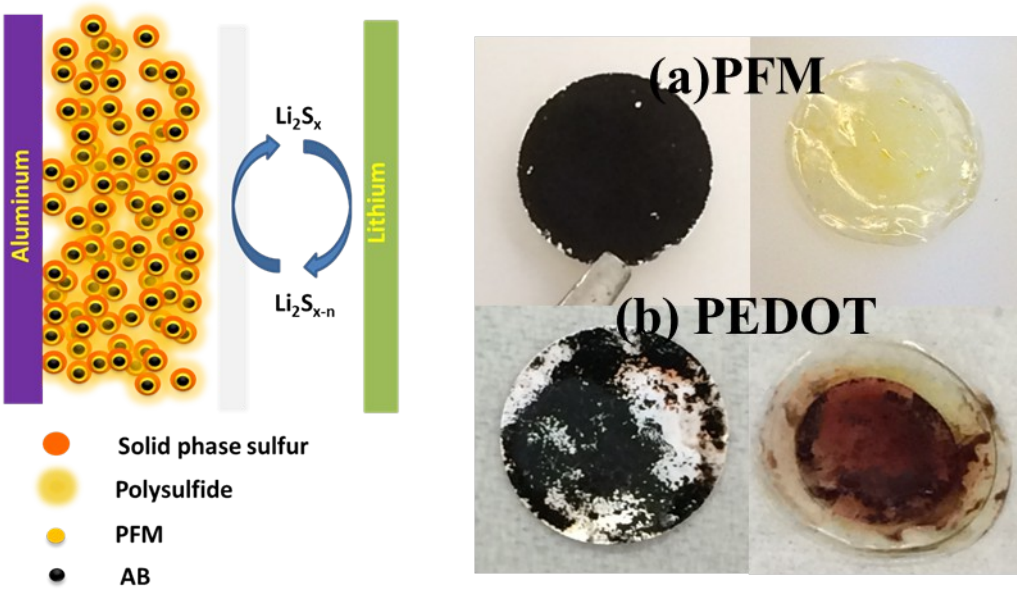

In this work, binders with different functional groups and conductivity in Li-S batteries were investigated. Solid sulfur species precipitation was observed with the assist of the carbonyl group, while a larger precipitation surface was obtained by incorporating conductive binders. This gave us a better understanding about the design of conductive binders for high-performance Li-S batteries.

Supporting information

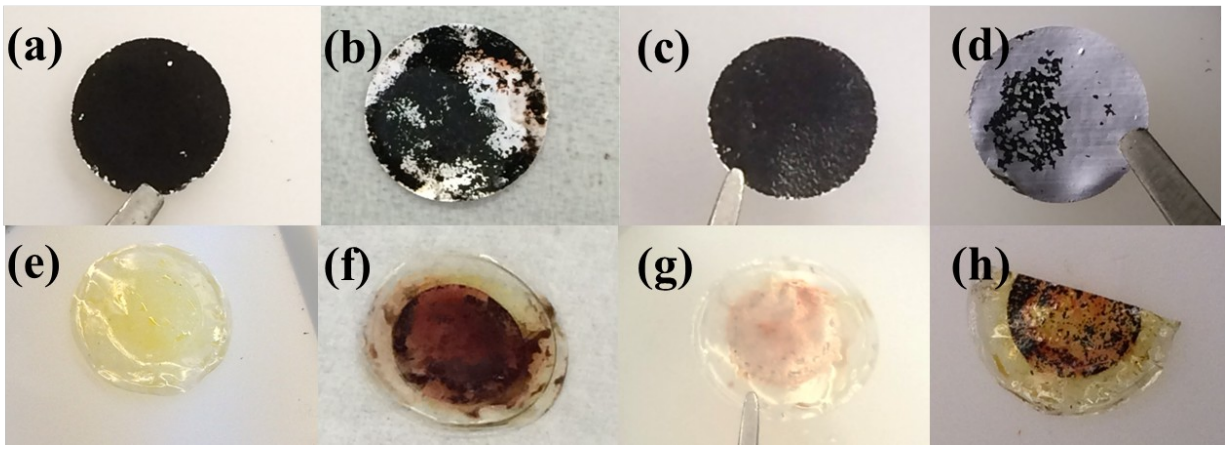

Figure S1. The photo image of the electrodes and spacers in disassembly cell with a different binder: PFM (a), (e); PEDOT (b), (f); PVP (c), (g); and PVDF (d), (h).